Research Article
Open Access

Swept-source optical coherence tomography assessment of the posterior cortical vitreous and choroidal thickness in different macular disorders

Abstract

Purpose: Swept-Source Optical Coherence Tomography (SS-OCT) determination of the prevalence of the Bursa Premacularis (BPM) and Space of Martegiani (SM) and assessment of Choroidal Thickness (CT) in healthy eyes (HE) and eyes with various macular disorders (MD).

Methods: Retrospective, comparative and non-interventional study. 134 non-consecutive patients underwent 1,050nm SS-OCT (DRI-OCT1 Atlantis®, Topcon Corp, and Japan). The prevalence of the BPM and SM was assessed in HE and MD patients. Macular CT was determined by measuring the distance between the RPE and the choroid/sclera junction at seven measurements (one subfoveal, three further determinations every 500µm up to 1500 µm temporal (T1, T2, T3) and nasal (N1, N2, N3) to fovea of 54 HE and 150 MD. Patients were categorised into 8 groups; (Diabetic Retinopathy (53), age-related macular degeneration (AMD) (32), High myopia (HM) (22), vitreomacular adhesion (VMA) and/or vitreomacular traction (VTM) (11), central serous retinopathy (CSR) (13), retinitis pigmentosa (RP) (9) and Miscellaneous (10).

Results: Mean age was 47±23 years for HE versus 57±22 years for MD ($p<0.05$). Mean sub-foveal CT was 289±75 µm for HE versus 223±84 µm for MD ($p=0.009$). BPM was detected in 36 out of 54 eyes of HE (66.7%); 95% confidence intervals (CI) [0.54-0.78] versus 51 out of 150 eyes (34.0%) of MD; 95% CI [0.27-0.41]; ($p=0.001$). SM was present in of 30 out of 54 eyes of HE (55.6%); 95% CI [0.42-0.68] versus 49 out of 150 eyes of MD (32.7%) ($p=0.004$). Sub-group analysis showed significant differences in CT between HE and MD with Diabetic Retinopathy, AMD, HM, CRS and VMA and/or VTM ($p<0.05$)

Conclusion: SS-OCT allows the measurement of CT in different macular anomalies and the assessment of the cortical vitreous and prevalence of the BPM and SM. The BPM and SM were more prevalent in HE. A thin choroid may be associated with Diabetic Retinopathy, AMD, High Myopia and VMA/VTM groups and a thick one with CSR group.

Keywords: swept-source optical coherence tomography, choroidal thickness, cortical vitreous, macular disorders, bursa premacularis, space of martegiani

Volume 5 Issue 3 - 2016

Pastor Idoate S,[1,2] Gil Martinez M,[1,2] Balaskas K,[1] Biswas S,[1,3] Stanga PE[1,2,3]
[1]Manchester Royal Eye Hospital, UK
[2]Manchester Vision Regeneration (MVR) Lab at NIHR/Wellcome Trust Manchester CRF, UK
[3]Manchester Academic Health Science Centre and Centre for Ophthalmology and Vision Research, University of Manchester, UK

Correspondence: Paulo E Stanga, Consultant Ophthalmologist & Vitreoretinal Surgeon, Professor of Ophthalmology & Retinal Regeneration, Manchester Royal Eye Hospital, Oxford Road, Manchester, M13 9WL, UK, Tel +441612765580, Fax +441612765642, Email retinaspecialist@btinternet.com

Received: October 30, 2016 | **Published:** November 28, 2016

Abbreviations: SS-OCT, swept-source optical coherence tomography; CT, choroidal thickness; MD, macular disorders; BPM, bursa premacularis; SM, space of martegiani; IRB, internal review board

Introduction

Optical coherence tomography (OCT) is a non-invasive, high-resolution technique capable of acquiring cross-sectional images of tissue morphology.[1] In ophthalmology, OCT is already a well-established clinical imaging method for the investigation of physiological properties and diseases of the eye.[2–4] The most common OCT imaging used today is spectral domain OCT (SD-OCT). Prior to the advent of SD-OCT, time-domain OCT (TD-OCT) ruled the day. SD-OCT is capable of operating nearly 100 times faster than TD-OCT. Operating at higher speeds permits acquisition of three-dimensional (3-D) data sets and simultaneous ultrahigh speed and ultrahigh resolution. These improvements result in images with more detailed information of the intraretinal layers, including the ganglion cell layer, photoreceptor layer, plexiform layers and nuclear layers. Nonetheless, due to the detection method used in SD-OCT, there is a fall-off in sensitivity with increasing depth in the eye, resulting in a lack of optimal outcomes in the sensitivity and in the quality of the image of the vitreous and the choroid in the same image.[5]

The main limitations to image in-vivo the vitreous body are its transparency and continuous movement. Besides, the vitreous fibers induce light-scattering with a secondary reduction in image contrast.[6] In addition, the presence of retinal pigment epithelium cells, which attenuate the incident light, preventing a proper assessment of choroidal changes, being therefore of limited diagnostic value in some conditions such as central serous chorioretinopathy (CSR), age-related macular degeneration (AMD), choroidal tumors or myopic maculopathies in which choroid plays a vital role in their pathophysiology.[7]

More recently, a new type of OCT methodology has been commercially introduced with Topcon's Deep Range Imaging (DRI)

OCT-1 Atlantis. This OCT instrument uses swept-source technology to overcome some of the more important weaknesses of SD-OCT. It's the fastest commercial OCT, with about 100,000 A-scans per second. Also, its 12mm wide scans allow us to capture the macular area and the disc in a single scan[8,9] It is now possible to image the vitreous, optic nerve, sclera and choroid all in one scan. Another feature of swept source OCT is that the light sources available generally operate in the 1 µm domain at 1,050 nm, which is a longer wavelength than SD-OCT one, which is usually around 840 nm[6,7,10–13] This increase in wavelength penetrates tissue better, and produces less scattering .The combination of these two technical characteristics allows for the improved visualization of the cortical vitreous and images deeper structures better[8–9] Hence, the aim of this study was to determine choroidal thickness and evaluate whether Swept-Source Deep Range Imaging Optical Coherence Tomography will provide improved *in vivo* anatomical characterization of the cortical vitreous in HE and patients with different MD.

Material and methods

Ethics statement

This is a retrospective study conducted according to the tenets of the Declaration of Helsinki. All patients gave informed consent to being imaged and for the collected data to be used for publication. The Manchester Royal Eye Hospital Steering Committee did not require for this retrospective study to undergo Internal Review Board (IRB) approval as all the imaging tests carried out were part of the routine care of patients.

Design and study population

A retrospective, comparative and non-interventional study was performed at Manchester Vision Regeneration (MVR) Laboratory at NIHR/Welcome Trust Manchester CRF/Manchester Royal Eye Hospital, UK. The macular area and posterior cortical vitreous of 134 non-consecutive patients who attended to Manchester Royal Eye Hospital were undergone to the 1,050nm SS-OCT system (DRI-OCT1 Atlantis®, Topcon Corp, and Japan). The prevalence of the Bursa Premacularis (BPM) and Space of Martegiani (SM) and Choroidal Thickness (CT) were assessed in HE and eyes with MD.

All scans were performed using the Topcon® SS-DRI-OCT. This system operates at a speed of 100,000 A-scans/second using a wavelength of 1,050nm produced by a wavelength tunable laser as a light source. The claimed axial resolution is 8 µm, the lateral resolution is 20 µm and the imaging depth in tissue is 2.3mm. Scans are averaged to reduce noise. The system is equipped with a tracking system to improve reproducibility. The 12mm long 5 raster lines cross pattern (5 lines vertical and 5 lines horizontal) default setting was used in a vitreous focal mode and centred on the fovea (Figure 1) to identify the presence or absence of a BPM, SM and measure the CT in each eye. The space among the top and the bottom line of the 5LineCross pattern was set at 1.5 mm.

Contrast and brightness of the images were digitally enhanced after collection to aid the delineation of anatomic features of the cortical vitreous. Macular CT was manually determined by measuring the distance between the RPE and the choroid/sclera junction by two independent observers, using the caliper system provided by the software. The images used for the measurements were the one with less retinal thickness crossing the centre of the fovea, to measure equivalent meridians in each patient. Seven measurements were taken: one subfoveal, three further determinations every 500µm temporal up to 1500µm (T1, T2, T3) and nasal (N1, N2, N3) to fovea (Figure 1) of 54 HE and 150 MD.

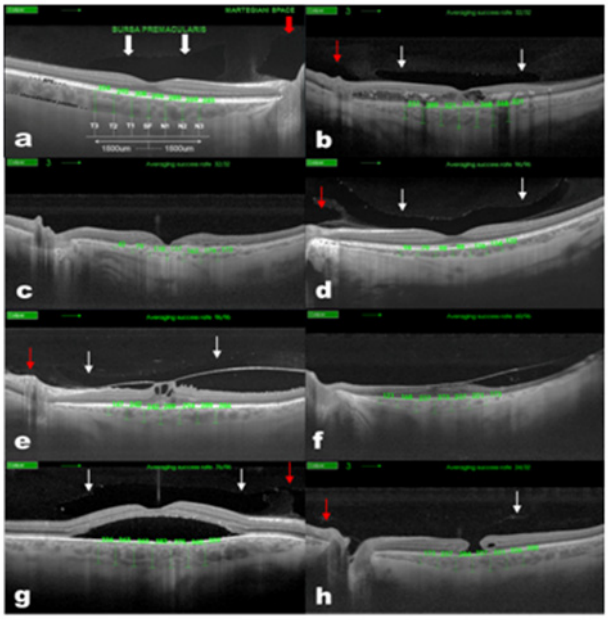

Figure 1 Choroidal thickness measurement in normal (A) Diabetic Retinopathy, (B) AMD, (C) myopic, (D) VMA and/or VTM, (E) RP, (F) CSR, (G) and miscellaneous, (H) patients. Swept-Source Deep Range Imaging Optical Coherence Tomography (SS-OCT) 5-lineCross raster scan demonstrating measurement technique used to obtain choroidal thickness across the macula. This OCT also demonstrates the presence of Bursa Premacularis (white arrows) and Martegiani space (red arrows).

Patients were categorised into 8 groups; (Diabetic Retinopathy (53), age-related macular degeneration (AMD) (32), high myopia (HM) (22), vitreomacular adhesion (VMA) and/or vitreomacular traction (VTM) (11), central serous retinopathy (CSR) (13), retinitis pigmentosa (RP) (9) and Miscellaneous (10). Patients with non-proliferative or proliferative diabetic retinopathy with or without diabetic macular edema were classified into the same group. AMD patients with the clinical diagnosis of either wet or dry were recruited in the same group. High myopia was defined as a spherical equivalent >5 diopters. Two observers determined choroidal thickness and the presence or absence of BPM and SM independently. The final thickness was calculated as the arithmetic mean of the calculations of two observers.

All statistical tests were performed using SPSS software version 16.0 for Windows (SPSS, Inc, Chicago, Illinois, USA). Kolmogorov-Smirnov test was used to identify the normality of the distribution, and then Student's t-test or Mann-Whitney U was performed for the CT among HE and MD. Also, the CT analysis among HE and different sub-groups was performed using Student's t-test or Mann-Whitney U test. The proportions of BPM and SM between HE and MD were analysed. Association was investigated using the Fisher's test. Pearson's correlation was used to correlate CT with age in HE and MD. A p value of <0.05 was considered statistically significant in this study. Miscellaneous group was only considered for the statistical analysis of the global sample (MD), but not for the subsequent analysis of the sub-groups due to heterogeneity in the retinal disorders of these patients.

Citation: Idoate PS, Martinez GM, Balaskas K, et al. Swept-source optical coherence tomography assessment of the posterior cortical vitreous and choroidal thickness in different macular disorders. *Adv Ophthalmol Vis Syst.* 2016;5(3):265–271. DOI: 10.15406/aovs.2016.05.00158

Results

The macular area of 150 MD eyes (classified in 8 sub-groups) was studied with an SS-OCT system and compared with 54 HE group. SS-OCT allowed visualization of CT in all (100%) sub-groups and also in the HE group (Figure 1). Mean age in HE group was 47±23 years (9-100) versus 57±22 years (6-92) in MD group (p<0.05 Student's t-test) (Table 1).

Table 1 Patient's Demographics and CT in Healthy Population and Macular Disorders Population

	Healthy Population	Macular Disorders Population	p-values
n (Eyes)	54	150	
Mean age; years	47±23	57±22	P<0.05; t-Student
Mean subfoveal CT	289±75	223±84	P<0.05; t-Student
Mean macular CT	252±32	193±24	P<0.05; U Mann Whitney
Subfoveal CT 95% CI	262.2-316.5µm	210.2-237.1µm	P<0.05
Macular CT 95% CI	240.1-263.5µm	189.8-197.1µm	P<0.05
Definite choroidal /sclera Junction, %	100	100	

CT, choroidal thickness; CI, confidence interval

Choroidal thickness

Mean sub-foveal CT was 289±75 µm (183-526) in HE versus 223±84 µm (26-405) in MD (p=0.009; 95% confidence interval (CI) [40.66-90.01]; Student's t-test). Average macular horizontal CT was 252±32 µm (196-289) in HE versus 193±28µm (154-223) in MD (p<0.05; U Mann Whitney) (Table 1). CT in HE was highest in the fovea (289 µm; CI 27.16 µm); then in the temporal side (251, 271, and 278 µm for T3, T2, and T1, respectively; confidence intervals (CIs) 23.12, 25.48, and 29.01 µm, respectively); and thinnest in the nasal side (253, 226, and 196 µm for N1, N2, and N3 respectively; CIs 31.18, 29.55, and 24.63 µm, respectively). CT in MD was highest in the fovea (223 µm; CI 13.48 µm); followed by the temporal (188, 203, 216 µm for T3, T2, and T1, respectively; CIs 11.81, 12.13, and 13.37 µm, respectively); and the nasal side (196,173, 154 µm for N1, N2, and N3 respectively; CIs 11.89, 10.70, and 13.17 µm, respectively) (Figure 2).

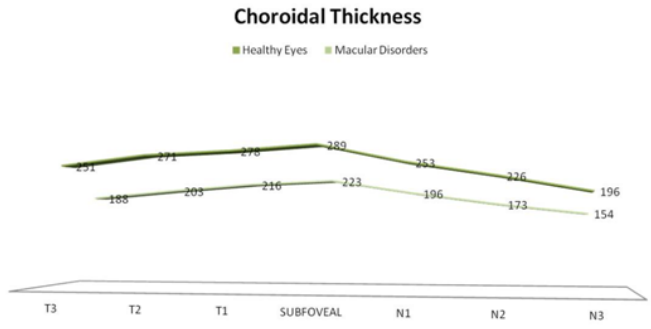

Figure 2 Graph showing the differences in macular choroidal thickness in healthy eyes group and macular disorders group. Mean thickness at each of the 7 locations measured at 500µm intervals temporal (T) and nasal (N) to the subfoveal area. The thickest choroid in healthy eyes group (top) and in the macular disorders group (bottom) was in foveal area and the thinnest in both groups was nasal (N3) area.

Differences in CT between both groups were statistically significant at T3, T2 and T1 (p<0.001 and p<0.001, p<0.001 respectively; 95% CIs [36.27-87.73], [44.85-91.15], [40.86-77.44], respectively; Student's t-test) and at nasal area at N1, N2 and N3 (p<0.001, p<0.001, p<0.001 respectively; 95% CIs [32.71-81.29], [30.92-75.08], [17.41-66.59], respectively; Student's t-test) (Figure 2). Pearson's correlation between CT and age in healthy and MD population was weak or not significant at fovea and nasal side. However, was significant at temporal side, T3, T2 and T1 (Figure 3).

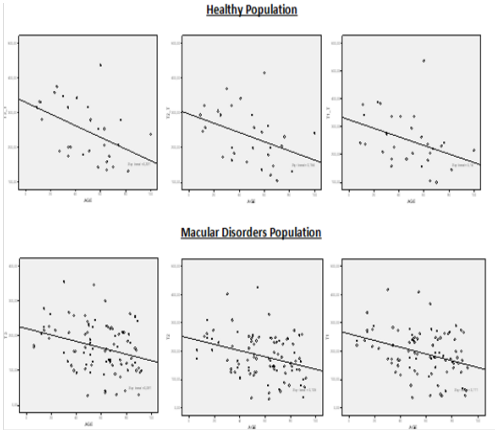

Figure 3 Scatter plot showing choroidal thickness at T3, T2 and T1 in the Healthy population and Macular disorders population. Choroidal thickness and age correlate significantly: (T3 (r=-0.475, p=0.009); T2 (r=-0.393, p=0.03); T1(r=-0.375, p=0.04) and T3 (r=-0.333, p=0.001); T2 (r=-0.323, p=0.002); T1(r=-0.302, p=0.004); respectively).

Posterior cortical vitreous

BPM was detected in 36 out of 54 eyes of HE (66.7%); CI [0.54-0.78] versus 51 out of 150 eyes (34.0%) of MD; CI [0.27-0.41]; (p=0.001 Fisher's test). SM was present in of 30 out of 54 eyes of HE (55.6%); CI [0.42-0.68] versus 49 out of 150 eyes of MD (32.7%) (p=0.004 Fisher's test). The BPM and SM coexisted in 24 out of 54 eyes of HE (44.0%) versus 40 out of 150 eyes (26.6%) of MD (p<0.05; Fisher's test) (Table 2).

Sub-group analysis

Sub-group analysis showed significant differences in CT between HE and MD with Diabetic Retinopathy, AMD, HM, CRS and VMA and/or ERM (p<0.05 U Mann Whitney) (Table 3).

Citation: Idoate PS, Martinez GM, Balaskas K, et al. Swept-source optical coherence tomography assessment of the posterior cortical vitreous and choroidal thickness in different macular disorders. *Adv Ophthalmol Vis Syst.* 2016;5(3):265–271. DOI: 10.15406/aovs.2016.05.00158

Table 2 Posterior Cortical Vitreous in Healthy Population and Macular Disorders Population

BPM/SM	Healthy Population	Macular Disorders Population	p-values
n (eyes)	54	150	
BPM	36(66.7%)	51(34.0%)	p=0.001; *Fisher Test*
SM	30 (55.6%)	49(32.7%)	p=0.009; *Fisher Test*
BPM+SM	24 (44.0%)	40 (26.6%)	p<0.05; *Fisher Test*

BPM, Bursa Premacularis; SM, Space of Martegiani

Table 3 Patients' Demographics and CT in Sub-groups and Healthy Population

Macular Disorders Population	n (eyes)	Mean age; years	p-value[1,2]	Mean subfoveal CT	p-value[1,2]	Mean horizontal macular CT	p-value[1,2]
Healthy Population	54	47±23		289±75 µm		252±32 µm	
Diabetic Retinopathy	53	54±16	P<0.0[1]	247±39 µm	p<0.0[1]	210±26 µm	p<0.0[2]
AMD	32	82±8	p<0.0[1]	181±50 µm	p<0.0[2]	158±18 µm	p<0.0[2]
High Myopia	22	57±23	p>0.0[2]	122±83 µm	p<0.0[2]	118±6 µm	p<0.0[2]
CSR	13	45±6	p>0.0[2]	396±55 µm	p<0.0[2]	344±46 µm	p<0.0[2]
VMA and/or VTM	11	67±23	p<0.0[2]	178±57 µm	p<0.0[2]	155±22 µm	p<0.0[2]
Retinitis Pigmentosa	9	45±21	p>0.0[2]	256±45 µm	p>0.0[2]	223±30 µm	p>0.0[2]
Miscellaneous	10	32±19	p>0.0[1]	---	---	---	---

AMD, aged related macular degeneration; CSR, central serous retinopathy; VMA and/or VTM, vitreomacular adhesion and/ or vitreomacular traction syndrome; CT, choroidal thickness; CI, confidence interval

1- t-student test

2- U Mann Whitney test

Diabetic Retinopathy

CT in Diabetic Retinopathy (Figure 4) was highest in the fovea (247 µm; CI 10.61 µm); then in the temporal side (201, 217, and 235 µm for T3, T2, and T1, respectively; CIs 11.0, 11.24, and 11.50 µm, respectively); and thinnest in the nasal side (215, 190 and 170 µm for N1, N2, and N3 respectively; CIs 11.89, 11.11 and 11.35 µm, respectively).

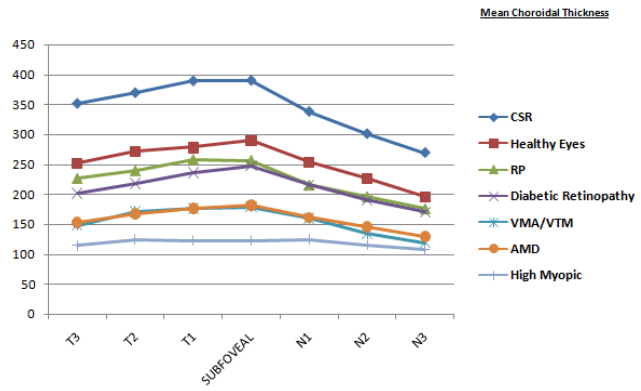

Figure 4 Graph showing the differences in macular choroidal thickness among healthy eyes group and different macular disorders groups. The thickest choroid in healthy eyes, CSR, Diabetic Retinopathy and VMA and/or VTM groups was in foveal area. The thickest choroid in RP, AMD and High Myopia eyes groups was in temporal 1 and foveal areas.

AMD

CT in AMD (Figure 4) was highest in temporal 1 and foveal areas (176, 181 µm for T1, CTSF respectively; CIs 20.29, 17.60 µm, respectively); then in the temporal 2 and nasal 1 sides (167, 161 µm for T2, N1 respectively; CIs 18.27, 17.18 µm, respectively); and thinnest in the temporal 3 and rest of nasal side (152, 145, and 129 µm for T3, N2 and N3 respectively; CIs 18.69, 15.66, and 15.44 µm, respectively).

High Myopia

CT in HM (Figure 4) was highest in the nasal1 and temporal 2 areas (124, 124 µm for N1, T2 respectively; CIs 35.81, 29.39 µm, respectively); then in the temporal 1 and foveal areas (123, 122 µm for T1, SFCT respectively; CIs 32,60, 34.85 µm, respectively); and thinnest in the nasal 2, 3 and temporal 3 sides (115, 107, and 114 µm for N2, N3, and T3 respectively; CIs 29.34, 27.83, and 32.60 µm, respectively).

CSR

CT in CSR (Figure 4) was highest in the fovea (396 µm; CI 30.34 µm); then in the temporal side (388, 369, and 351 µm for T3, T2, and T1, respectively; CIs 28.21, 31.86, and 28.33 µm, respectively); and thinnest in the nasal side (337, 300 and 269 µm for N1, N2, and N3 respectively; CIs 40.76, 44.12, and 36.56 µm, respectively).

VMA and/or VTM

CT in VMA and/or VTM (Figure 4) was highest in the fovea (178 µm; CI 34.41 µm); then in the temporal side (176, 170, and 147 µm for T3, T2, and T1, respectively; CIs 40.26, 38.23, and 34.58 µm, respectively); and thinnest in the nasal side (159, 134 and 119 µm for N1, N2, and N3 respectively; CIs 34.50, 31.67, and 29.05 µm, respectively).

RP

CT in RP (Figure 3) was highest in temporal 1 and foveal areas (256, 257 µm for T1, CTSF respectively; CIs 30.30, 29.94 µm, respectively); then in the rest of temporal side (239, 226 µm for T2, T3 respectively; CIs 30.15, 38.25 µm, respectively); and thinnest in the nasal side (215, 195, and 175 µm for N1, N2 and N3 respectively; CIs 22.46, 26.07, and 32.53 µm, respectively).

Posterior cortical vitreous in sub-groups

Sub-group analysis showed significant differences in BPM and SM between HE and MD with Diabetic Retinopathy, AMD, HM, VMA and/or VTM ($p<0.05$; Fisher's test) (Table 4). The BPM and SM coexisted in 18 out of 53 eyes of Diabetic Retinopathy (33.9%), 7 out of 22 eyes of HM (31.8%), 5 out of 13 eyes of CSR (38.5%), 2 out of 11 eyes of VMA and/or VTM (18.8%) and in 4 out of 9 eyes of RP (44.4%). Significant differences were found between HE and MD with AMD and VMA and/or VTM ($p<0.05$; Fisher's test) (Table 4).

Table 4 Posterior cortical vitreous in sub-groups and healthy population

Macular Disorders Population	n (eyes)	p-values	BPM	SM	p-values	BPM+SM	p-values
Healthy Population	54	36(66.7%)		30 (55.6%)		24 (44.0%)	
Diabetic Retinopathy	53	22(41.5%)	P<0.05	24(45.3%)	P>0.05	18(33.9%)	P>0.05
AMD	32	2(6.3%)	P<0.05	(0%)	P<0.05	(0%)	P<0.05
High Myopia	22	9(40.9%)	P<0.05	8(36.4%)	P>0.05	7(31.8%)	P>0.05
CSR	13	5(38.5%)	P>0.05	8(61.5%)	P>0.05	5(38.5%)	P>0.05
VMA and/or VTM	11	3(27.3%)	P<0.05	2(18.8%)	P<0.05	2(18.8%)	P<0.05
Retinitis Pigmentosa	9	5(55.5%)	P>0.05	5(55.5%)	P>0.05	4(44.4%)	P>0.05
Miscellaneous	10	4(40.0%)	---	4(40.0%)	---	4(40.0%)	---

AMD, aged related macular degeneration; CSR, central serous retinopathy; VMA and/or VTM, vitreomacular adhesion and/or vitreomacular traction syndrome; BPM, bursa premacularis; SM, space of martegiani

Discussion

Until recently, indocyanine green angiography was the best diagnostic test for diseases involving the choroidal circulation and anatomy[14,15] but recent advances in OCT technology have added cross-sectional information about the choroid[7] The images provided by SD-OCT was a prompt revolution in the ability to image the choroid, increasing the knowledge about the pathophysiology and etiology of several ocular conditions,[16-23] but recently, long wavelength SS-OCT system provides higher penetration through the RPE, enabling deep choroidal imaging, and generating an uniform image quality of all anatomic structures distributed between the cortical vitreous to the anterior surface of the sclera at the same scan image.

The combination of higher wavelength and higher scanning speed software with less scatter allows for improved *in vivo* anatomic characterization of structures of the posterior cortical vitreous such as the Bursa Premacularis and Martegiani Space and image deeper structures better, overcoming RPE barrier effect and movement artefacts.[6,24] Long wavelength SS-OCT was employed to measure the CT. Visualization of Choroid-Scleral junction has been satisfactory in both, control and MD groups (100%), as same as, it has been reported in other study with SS-OCT,[24] and better or comparable to the reported in previous studies, using Cirrus, Spectralis or RTVue.[7,18,25] In addition, the control group's values showed data comparable to previous studies[7,18,24,26] in mean age, subfoveal CT and correlation between CT and age (25), with a significant inverse correlation between CT and age in HE and MD (Figure 3).

However, the age factor should be carefully considered in our series, because of we have compared populations with different age distribution (Tables 1&2). Although, a significant correlation like previous series (24) was found between CT in temporal side and age (T3 (r=-0.475, p=0.009); T2 (r=-0.393, p=0.03); T1(r=-0.375, p=0.04), the age at which subfoveal choroidal thickness starts to decrease is still to be determined.[27] Mean subfoveal CT in our HE group (289±75µm) was lower than the average values reported in other studies of CT with SS-OCT. It could be due to our cohort of patients included a wide range of ages (9-100). The topographic profile of CT in HE in our series (Figure 2) was highest in subfoveal area, followed by the temporal and the nasal areas, as has been previously reported in other series.[7,18,21,24,27]

It has been previously reported that changes in CT are associated with some ocular conditions such as CSR[16,17] AMD[18,19] and HM.[21,23] Also, differences in CT have been reported in patients with diabetic retinopathy comparing to normal population.[25] We found significant differences in our series, in CT between HE and MD with Diabetic Retinopathy, AMD, HM, CRS and VMA and/or VTM (Table 1&2). The Means subfoveal (Figure 4) in Diabetic retinopathy (247±39µm), and RP (256±45µm) were higher than the average values reported in other series,[28–30] in HM (122±83µm) was comparable to the reported in previous studies,[21,31] and in AMD and CSR (181±50µm, 396±55µm; respectively) were lower than the average values reported in other series.[16–19] Mean subfoveal CT in our VMA and/or VTM group was (178±57µm) lower than the AMD group. Mean age (67±23 years) was also lower than the AMD group. This data should be carefully considered. Firstly, the sample size of this group (11 eyes), maybe is too small to draw out absolute conclusions about the CT in this condition and secondly, lack of previously reported series to compare our results in this condition Thus, further studies are required to better understand the role of CT in this eye condition.

Citation: Idoate PS, Martinez GM, Balaskas K, et al. Swept-source optical coherence tomography assessment of the posterior cortical vitreous and choroidal thickness in different macular disorders. *Adv Ophthalmol Vis Syst.* 2016;5(3):265–271. DOI: 10.15406/aovs.2016.05.00158

The topographic profile of CT in MD groups in our series (Figure 4) was highest in subfoveal area, followed by the temporal and the nasal areas in Diabetic Retinopathy, AMD, VMA and/or VTM and CSR as has been previously reported in other series. In contrast, mean temporal 1 CT values were higher than the subfoveal in HM and RP groups. *In vivo* imaging of the vitreous body has to date been difficult owing to its transparency and movement. Higher scanning speeds compensate for the movement of the vitreous fibers while the longer wavelength induces less light scattering by the vitreous fibers. The combination of these developments allows for the imaging the features of the posterior cortical vitreous.

In our series, the overall prevalence of BPM and SM detected in healthy population was (66.7% and 55.6%, respectively), comparable to values reported in previous studies.[6,32] In the MD sample was (34% and 32, 7%; respectively) lower than in the healthy population. Also we found significant differences among the different MD conditions comparing with the eyes of healthy population. Unfortunately, we have no previous reported series to compare with our series. The BPM and SM represent points of weakness in the cortical vitreous. Therefore, these results could suggest that posterior cortical vitreous could be also affected in of some ocular conditions.

Interestingly, there have been several recent studies that support the idea that posterior cortical vitreous might be associated with the development and progression of exudative AMD.[33–36] In our series, we could not find any evidence of SM in AMD patients. In addition, the prevalence of BPM was 6.3%. Vitreous synchysis is postulated to be the main factor responsible for the reduced prevalence of detected BPM.[37,38] However, AMD patients with the clinical diagnosis of either wet or dry were recruited in the same group in this study, and the percentage of patients with dry AMD was superior to wet AMD patients. Thus; further studies with this technology are needed to clarify the role of posterior cortical vitreous in wet-AMD development.

There are some limitations to this study. This study is a retrospective review of non-consecutive patients who already carried the diagnoses of Diabetic Retinopathy, AMD, HM, VMA and/or VTM, CSR and RP. Lacking of strict inclusion criteria, heterogenous population are two strong limitations. Patients were excluded from this study if full CT was unable to be visualized adequately to perform the 7 measurements as described above. The Miscellaneous group was constituted with many different ocular conditions such as traumatic macular holes, retinal detachments, optic pit maculopathy or coats diseases), forming a heterogeneous sample group. Despite its small number of subjects (10), maybe, they could have interfered with the final results in the CT of the MD sample. The number of eyes in some MD groups could be not enough appropriate to draw out absolute conclusions. In this study, only the presence or absence of BPM and SM has been identified, therefore any other abnormalities in macular disorders that could have a role in the pathogenesis of these diseases have not been reported.

In addition, we may mention that CT has to be manually determined by 2 independent observers, since there is no commercially available automated software, and maybe it has limited the accuracy of the measurements. But despite of these limitations, to the best of our knowledge, this is the first report of assessment of posterior cortical vitreous and choroidal thickness in different macular disorders at the same time, comparing with healthy population. According to our results, macular CT is higher in healthy eyes than in the MD sample with different CT profiles, suggesting that changes in CT could play an important role in the pathogenesis of some ocular conditions. In the other hand further studies are required to better understand the role of BPM and SM in these different eye conditions and perhaps their influence on the response to intravitreal therapies.

Funding

None.

Acknowledgments

None.

Conflicts of interest

The authors declare that there was no conflict of interest.

References

1. Huang D, Swanson EA, Lin CT, et al. Optical coherence tomography. *Science*. 1991;254(5035):1178–1181.
2. Coscas F, Querques G, Forte R, et al. Combined fluorescein angiography and spectral–domain optical coherence tomography imaging of classic choroidal neovascularization secondary to age–related macular degeneration before and after intravitreal ranibizumab injections. *Retina*. 2012;32(6):1069–1076.
3. Vermeer KA, van der Schoot J, Lemij HG, et al. RPE–normalized RNFL attenuation coefficient maps derived from volumetric OCT imaging for glaucoma assessment. *Invest Ophthalmol Vis Sci*. 2012;53(10):6102–6108.
4. Baskin DE. Optical coherence tomography in diabetic macular edema. *Curr Opin Ophthalmol*. 2010;21(3):172–177.
5. de Bruin DM, Burnes DL, Loewenstein J, et al. *In vivo* three–dimensional imaging of neovascular age–related macular degeneration using optical frequency domain imaging at 1050 nm. *Invest Ophthalmol Vis Sci*. 2008;49(10):4545–4552.
6. Stanga PE, Sala–Puigdollers A, Caputo S, et al. *In Vivo* Imaging of Cortical Vitreous Using 1050–nm Swept–Source Deep Range Imaging Optical Coherence Tomography. *Am J Ophthalmol*. 2014;157(2):397–404.
7. Branchini L, Regatieri CV, Flores–Moreno I, et al. Reproducibility of choroidal thickness measurements across three spectral domain optical coherence tomography systems. *Ophthalmology*. 2012;119(1):119–123.
8. Matsuo Y, Sakamoto T, Yamashita T, et al. Comparisons of choroidal thickness of normal eyes obtained by two different spectral–domain OCT and one swept–source OCT instruments. *Invest Ophthalmol Vis Sci*. 2013;54(12):7630–7636.
9. Pedinielli A, Souied E, Perrenoud F, et al. *In vivo* visualization of perforating vessels and focal scleral ectasia in pathologic myopia. *Invest Ophthalmol Vis Sci*. 2013;54(12):7637–7643.
10. Huber R, Adler DC, Srinivasan VJ, et al. Fourier domain mode locking at 1050 nm for ultra–high–speed optical coherence tomography of the human retina at 236,000 axialscans per second. *Opt Lett*. 2007;32(14):2049–2051.
11. Lim H, de Boer JF, Park BH, et al. Optical frequency domain imaging with a rapidly swept laser in the 815–870 nm range. *Opt Express*. 2006;14(13):5937–5944.
12. Unterhuber A, Povazay B, Hermann B, et al. *In vivo* retinal optical coherence tomography at 1040 nm – enhanced penetration into the choroid. *Opt Express*. 2005;13(9):3252–3258.
13. Yasuno Y, Hong Y, Makita S, et al. *In vivo* high–contrast imaging of deep posterior eye by 1–micron swept source optical coherence tomography and scattering optical coherence angiography. *Opt Express*. 2007;15(10):6121–6139.

14. Stanga PE, Lim JI, Hamilton P. Indocyanine green angiography in chorioretinal diseases: indications and interpretation: an evidence–based update. *Ophthalmology*. 2003;110(1):15–21.

15. Yannuzzi LA. Indocyanine green angiography: a perspective on use in the clinical setting. *Am J Ophthalmol*. 2011;151(5):745–751.e1.

16. Imamura Y, Fujiwara T, Margolis R, et al. Enhanced depth imaging optical coherence tomography of the choroid in central serous chorioretinopathy. *Retina*. 2009;29(10):1469–1473.

17. Maruko I, Iida T, Sugano Y, et al. Subfoveal choroidal thickness in fellow eyes of patients with central serous chorioretinopathy. *Retina*. 2011;31(8):1603–1608.

18. Manjunath V, Goren J, Fujimoto JG, et al. Analysis of choroidal thickness in age–related macular degeneration using spectral–domain optical coherence tomography. *Am J Ophthalmol*. 2011;152(4):663–668.

19. Switzer DW, Mendonca LS, Saito M, et al. Segregation of ophthalmoscopic characteristics according to choroidal thickness in patients with early age–related macular degeneration. *Retina*. 2012;32(7):1265–1271.

20. Nakai K, Gomi F, Ikuno Y, et al. Choroidal observations in Vogt–Koyanagi–Harada disease using high–penetration optical coherence tomography. *Graefes Arch Clin Exp Ophthalmol*. 2012;250(7):1089–1095.

21. Flores–Moreno I, Lugo F, Duker JS, et al. The relationship between axial length and choroidal thickness in eyes with high myopia. *Am J Ophthalmol*. 2013;155(2):314–319.

22. Say EA, Shah SU, Ferenczy S, et al. Optical coherence tomography of retinal and choroidal tumors. *J Ophthalmol*. 2011:385058.

23. Fujiwara T, Imamura Y, Margolis R, et al. Enhanced depth imaging optical coherence tomography of the choroid in highly myopic eyes. *Am J Ophthalmol*. 2009;148(3):445–450.

24. Ruiz–Moreno JM, Flores–Moreno I, Lugo F, et al. Macular choroidal thickness in normal pediatric population measured by swept–source optical coherence tomography. *Invest Ophthalmol Vis Sci*. 2013;54(1):353–359.

25. Ho J, Branchini L, Regatieri C, et al. Analysis of normal peripapillary choroidal thickness via spectral domain optical coherence tomography. *Ophthalmology*. 2011;118(10):2001–2007.

26. Margolis R, Spaide RF. A pilot study of enhanced depth imaging optical coherence tomography of the choroid in normal eyes. *Am J Ophthalmol*. 2009;147(5):811–815.

27. Regatieri CV, Branchini L, Carmody J, et al. Choroidal thickness in patients with diabetic retinopathy analyzed by spectral–domain optical coherence tomography. *Retina*. 2012;32(3):563–568.

28. Esmaeelpour M, Považay B, Hermann B, et al. Mapping Choroidal and Retinal Thickness Variation in Type 2 Diabetes using Three–Dimensional 1060–nm Optical Coherence Tomography. *Invest Ophthalmol Vis Sci*. 2011;52(8):5311–5316.

29. Regatieri CV, Branchini L, Carmody J, et al. Choroidal thickness in patients with diabetic retinopathy analyzed by spectral–domain optical coherence tomography. *Retina*. 2012;32(3):563–568.

30. Ayton LN, Guymer RH, Luu CD. Choroidal thickness profiles in retinitis pigmentosa. *Clin Experiment Ophthalmol*. 2013;41(4):396–403.

31. Nishida Y, Fujiwara T, Imamura Y, et al. Choroidal thickness and visual acuity in highly myopic eyes. *Retina*. 2012;32(7):1229–1236.

32. Mojana F, Kozak I, Oster SF, et al. Observations by spectral–domain optical coherence tomography combined with simultaneous scanning laser ophthalmoscopy: imaging of the vitreous. *Am J Ophthalmol*. 2010;149(4):641–650.

33. Robison CD, Krebs I, Binder S, et al. Vitreomacular adhesion in active and end–stage age–related macular degeneration. *Am J Ophthalmol*. 2009;148(1):79–82.

34. Lee SJ, Lee CS, Koh HJ. Posterior vitreomacular adhesion and risk of exudative age–related macular degeneration: paired eye study, *Am J Ophthalmol*. 2009;147(4):621–626.

35. Mojana F, Cheng L, Bartsch DU, et al. The role of abnormal vitreomacular adhesion in age–related macular degeneration: spectral optical coherence tomography and surgical results, *Am J Ophthalmol*. 2008;146(2):218–227.

36. Krebs I, Glittenberg C, Zeiler F, et al. Spectral domain optical coherence tomography for higher precision in the evaluation of vitreoretinal adhesions in exudative age–related macular degeneration, *Br J Ophthalmol*. 2011;95(10):1415–1418.

37. Itakura H, Kishi S. Aging changes of vitreomacular interface. *Retina*. 2011;31(7):1400–1404.

38. Le Goff MM, Bishop PN. Adult vitreous structure and postnatal changes. *Eye*. 2008;22(10):1214–1222.

Citation: Idoate PS, Martinez GM, Balaskas K, et al. Swept-source optical coherence tomography assessment of the posterior cortical vitreous and choroidal thickness in different macular disorders. *Adv Ophthalmol Vis Syst.* 2016;5(3):265–271. DOI: 10.15406/aovs.2016.05.00158